2 October 1998

ELSEVIER

Chemical Physics Letters 295 (1998) 113–121

CHEMICAL PHYSICS LETTERS

A three-dimensional quantum mechanical study of the $O + HO_2$ atmospheric reaction: infinite-order sudden approximation and novel adiabatic approaches vs. quasiclassical trajectories

A.J.C. Varandas *, H. Szichman

Departamento de Química, Universidade de Coimbra, 3049 Coimbra Codex, Portugal

Received 1 July 1998; revised 27 July 1998

Abstract

We present a quantum mechanical, three-dimensional infinite-order-sudden-approximation study of the $O + HO_2$ reaction using a recently reported HO_3 double many-body expansion potential energy surface. The reaction is treated as coplanar, for which a 3D treatment represents still a reduced dimensionality analysis. The results are compared with experimental data and previously reported quasiclassical trajectory calculations which employed the same potential. Novel adiabatic approaches have also been developed. In comparison with the trajectory calculations and experiment, the agreement of the adiabatic results is good. Striking deficiencies are noted for the sudden approximation near the reaction threshold. © 1998 Elsevier Science B.V. All rights reserved.

1. Introduction

We have carried out a 3D quantum mechanical (QM) study of the important atmospheric reaction

$$O + HO_2 \rightarrow OH + O_2,$$

$$\Delta H_{\text{class}} = -51.94\,\text{kcal}\,\text{mol}^{-1}. \quad (1)$$

where ΔH_{class} is the classical enthalpy of reaction. All calculations employed a recently reported single-valued double many-body expansion (DMBE) potential energy surface for the electronic ground state of HO_3 [1]. Such a reaction has been studied experimentally by several groups [2–7] due to its key role in atmospheric chemistry. It has also been the subject of a quasiclassical trajectory (QCT) simulation [8].

The present calculations have been carried out by considering only the nonreactive arrangement channel (AC) [9]. Thus, our methods are able to yield integral total reactive probabilities, but fail to have the capability of discerning between the different output channels (which is of no practical importance for the title reaction; see later). However, they have a significant advantage over other methods in that the calculations can be performed without having to invoke transformations of coordinates. Additionally, the number of energy states involved in the computations is minimal, compared with detailed state-to-state reactive probability calculations. Treating only one AC becomes even more convenient if approxima-

* Corresponding author.

0009-2614/98/$ - see front matter
PII: S0009-2614(98)00925-7

tions are to be applied. Among these are the coupled states (or j_z) [10,11] and the infinite-order sudden approximation [11] (IOSA) methods.

In the coupled states approximation, the Coriolis interactions [11,10], which are responsible for the coupling of overall to internal rotations, are neglected ad hoc. It is clear that the effect of such an approximation will be smaller in a single AC system than for three ACs, a situation that one would need to consider in a detailed state-to-state reactive probability calculation.

The IOSA is a multidimensional approximation which is based on the assumption that the reaction happens in a very small time interval, such that the different directional parameters do not vary appreciably during the collisional process. In such conditions, the rotational elements can be neglected, reducing the dimensionality of the mathematical description of the reactive process. This approximation should be acceptable for high translational energies, as the collisional period varies as $\tau \approx E_{\rm tr}^{-1}$. Moreover, it should be better for heavy target molecules and light colliding particles, since heavy targets, being characterized by a large inertial moment, would find it difficult to change direction in a short time interval. Nevertheless, even if the role of energy and mass can be easily assessed in the IOSA model, the importance of boundary conditions, such as geometry factors, which prevail in the molecule at the moment of the interaction is not self-evident. Since this approximation does not explicitly refers to them, there may be a lot of modelling options to be applied and only an a posteriori comparison of the computed results with the experimental data or more accurate theoretical results may indicate which is most appropriate. We have some experience with the IOSA in this respect. From the cases that we have considered, we have found that in applying it to systems like HHOH [12] and O_4 [13,9], it yielded reasonable results. However, in some other studies done for the systems HNNO [14] and more recently HO_3 [15,16], the results have been less satisfactory, with the IOSA method leading systematically to much lower values for the calculated cross sections near the threshold than those obtained from QCT simulations; such differences were partly attributed to the problem of zero-point energy leakage in classical dynamics [15,16] and partly to deficiencies in the quantum mechanical approach. In summary, the calculated QM values of the rate constants tend to be systematically underestimated.

In this respect, it is of importance to continue assessing the IOSA model in elementary processes such as the title reaction, since they are known to yield large experimental rate coefficients [4–7]. In addition, taking into account the difficulties encountered in analyzing the title reaction by the IOSA method, we suggest a novel model which is based on an adiabatic path approach and seems to gap the differences between the QCT and IOSA models for the title reaction.

2. Theory

As described elsewhere [9,12–14], our method is based on the calculation of all non-reactive probabilities, i.e. $\boldsymbol{P}(\lambda \leftarrow \lambda_0)$, the sum of which is then subtracted from unity to obtain the total reactive probability. Thus, we write

$$P_{\rm react} = 1 - \sum_{\lambda} |S(\lambda \leftarrow \lambda_0)|^2 \tag{2}$$

where $S(\lambda \leftarrow \lambda_0)$ is an inelastic state-to-state S matrix element and λ (and λ_0) stand for a set of quantum numbers which label a state of the four-atom system.

The matrix element $S(\lambda \leftarrow \lambda_0)$ can be written as

$$S(\lambda \leftarrow \lambda_0) = \left[\delta_{\lambda\lambda_0} - \frac{1}{i\hbar} \langle \psi_\lambda | V | (\chi_{\lambda_0} + \psi_{\lambda_0}) \rangle \exp(i\phi_\lambda) \right] \tag{3}$$

where $\delta_{\lambda\lambda_0}$ is the Kronecker delta function and ϕ_λ is the (elastic) λ-th phase shift.

In Eq. (3), ψ_λ represents the λ-th quantum mechanical solution of an unperturbed (elastic) Schrödinger equation, namely

$$(E - H_0)\,\psi_\lambda = 0 \tag{4}$$

In turn, χ_{λ_0} can be obtained by solving the following inhomogeneous Schrödinger equation in the close-interaction region

$$(E - H_I)\,\chi_{\lambda_0} = V\psi_{\lambda_0} \tag{5}$$

where V is an interaction (perturbation) potential defined by

$$V = H - H_0 \tag{6}$$

Thus, H is the full Hamiltonian and H_I is ad hoc obtained by adding to H negative imaginary potentials (NIPs); these are defined along the boundaries of the arrangement channel in which ψ_λ is calculated. As usual, the function of these NIPs is to decouple one arrangement channel from all others and provide bound-state like boundary conditions [17].

As illustrated in Fig. 1, a Jacobi coordinate system has been used in the present work to describe both AC's of the four-atom system. Thus, the atom-triatom (reagent) channel is described by three radial distances and three Jacobi angles. The former include the vibrational coordinate for the unbroken bond r, the corresponding ''translational'' coordinate of the triatom ρ connecting the third atom with the center of mass of the unbroken bond, and the translational coordinate R which connects the fourth atom to the center of mass of the triatomic system. Three Jacobi angles then complete the description of the system: θ (the angle between r and ρ); γ (the angle between ρ and R); and β (the polar angle between the triatom plane and R). The calculations reported here are also characterized by the use of the following 5D polar angle-averaged potential energy surface

$$\bar{U}(r\rho R\theta\gamma) = \frac{1}{\pi}\int_0^\pi U(r\rho R\theta\gamma\beta)\,\mathrm{d}\beta. \tag{7}$$

In order to calculate ψ_λ (and χ_{λ_0}) within the IOSA approach, the following Hamiltonian should be considered [18]

$$H = -\frac{\hbar^2}{2m}\frac{\partial^2}{\partial r^2}r - \frac{\hbar^2}{2\mu\rho}\frac{\partial^2}{\partial\rho^2}\rho - \frac{\hbar^2}{2MR}\frac{\partial^2}{\partial R^2}R + \left(\frac{1}{2\mu\rho^2} + \frac{1}{2mr^2}\right)J^2 + \frac{\hbar^2 J(J+1)}{2MR^2} + \bar{U}(r\rho R\theta\gamma) \tag{8}$$

where the averaged potential energy surface has been used and m, μ and M are respectively the reduced masses of the diatomic bond (OH in the present case), the triatomic molecule and the whole atom + triatom system. Moreover, J represents the bending angular momentum operator of the triatomic molecule and J is the total angular momentum quantum number. It should be noted that a term of the form

$$\left(\frac{1}{2\mu\rho^2} + \frac{1}{2MR^2}\right)\boldsymbol{K}^2(\gamma) \tag{9}$$

representing the rotational angular momentum of the triatomic molecule has been omitted in Eq. (8), since in the IOSA model we consider γ as a parametric coordinate (i.e., calculations are done for fixed values of γ).

In general we distinguish between the asymptotic region and the short interaction region. The Schrödinger equation that follows by employing the Hamiltonian defined in Eq. (8) is treated twice: once to calculate the asymptotic (unperturbed) elastic wavefunction ψ_λ and once to calculate χ_{λ_0}. In this paragraph we start by considering the expression of the (unperturbed) potential energy surface to be used for the solution of ψ_λ [see Eq. (4)]. It is given by

$$\bar{U}(r\rho R\theta\gamma) = v(r\rho\theta) + w(R\gamma) \tag{10}$$

where $v(r\rho\theta)$ is the potential energy surface of the HO_2 molecule which follows from

$$v(r\rho\theta) = \lim_{R\to\infty} U(r\rho R\theta\gamma\beta) \tag{11}$$

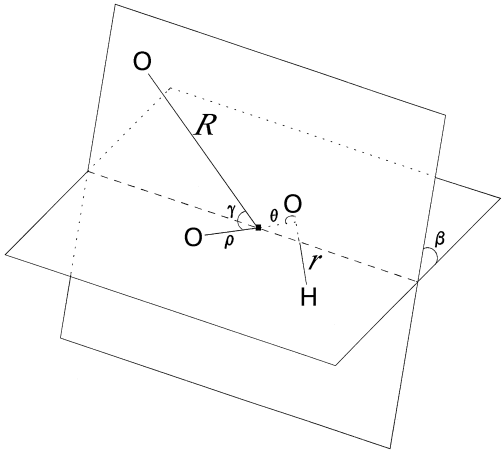

Fig. 1. Schematic representation of the Jacobi coordinate system employed for the calculations in the present work. Note that ρ is the vector connecting one of the O atoms in HO_2 to the center of mass of the remaining OH.

and the distortion potential $w(R\gamma)$ is defined by

$$w(R\gamma) = \overline{U}(R\rho_e r_e \theta_e \gamma) \tag{12}$$

Note that ρ_e, r_e and θ_e are obtained from the equilibrium properties of the HO_2 [19] triatomic molecule, which is an integral part of the HO_3 potential energy surface [1], while γ is the IOSA angle [12,15,9].

The function χ_{λ_0} is derived by solving Eq. (5) in the reagents AC. For that purpose the range of the reagents vibrational coordinate(s) are enlarged so as to comprise the relevant reactive regions and include the necessary decoupling NIPs. In the title reactive system, there is only one open channel [8] and consequently the bond OH in the HO_2 molecule remains unbroken through all the reactive process. In order to account for this possibility, two negative imaginary terms are added to the real Hamiltonian: a vibrational term along the distance ρ and another translational term along R, namely

$$V_I(r,\rho,R) \equiv -i\left[v_{I\rho}(\rho) + v_{IR}(R)\right] \tag{13}$$

The addition of the NIPs to the real averaged potential $\overline{U}$ converts the scattering problem into a bound system problem and hence makes χ_{λ_0} expandable in terms of square integrable L^2 functions [20,21]. These functions are chosen here as localized functions for the translational components and adiabatic basis sets for the vibrational ones. Thus,

$$\chi^J_{\lambda_0}(r\rho R\theta\gamma|j) = \frac{1}{r\rho R}\sum_{n\lambda} a^J_{n\lambda}\, g(R|n)\, f(r\rho\theta\gamma|j|n\lambda) \tag{14}$$

where $g(R|n)$ represents the translational component which is chosen to be a standard Gaussian function of the form

$$g(R|n) = \left(\frac{\alpha}{\sigma\sqrt{\pi}}\right)^{1/2} \exp\left[-\frac{\alpha^2}{2}\left(\frac{R-R_n}{\sigma}\right)^2\right] \tag{15}$$

where σ is the translational step size

$$\sigma = R_n - R_{n-1} \tag{16}$$

Regarding $f(r\rho\theta\gamma|j|n\lambda)$, this is an eigenfunction of the 3D Schrödinger equation

$$\left[-\frac{\hbar^2}{2mr}\frac{\partial^2}{\partial r^2}r - \frac{\hbar^2}{2\mu\rho}\frac{\partial^2}{\partial\rho^2}\rho + \left(\frac{1}{2mr^2} + \frac{1}{2\mu\rho^2}\right)J^2 + \overline{U}(r\rho R_n\theta\gamma) - \epsilon(\lambda|\theta\gamma j|R_n)\right] \times f(r\rho\theta\gamma|j|n\lambda) = 0 \tag{17}$$

Once Eq. (17) has been solved, it is then possible, starting from Eq. (7), to obtain the γ-dependent S-matrix element. Finally, to obtain the reactive probabilities, the following average is required

$$\langle|S^J(\lambda\leftarrow\lambda_0)|^2\rangle = \frac{1}{2}\int_{-1}^{1}|S^J(\lambda\leftarrow\lambda_0)\big|_\gamma|^2 \mathrm{d}\cos\gamma \tag{18}$$

From the J-specific averaged reaction probabilities, one then gets the QM total reactive cross sections by using

$$\sigma^r(E_{\mathrm{tr}},\lambda_0) = \frac{\pi}{k^2(E_{\mathrm{tr}})}\sum_J (2J+1)\,P^J_{\mathrm{react}}(E_{\mathrm{tr}},\lambda_0) \tag{19}$$

where $k(E_{\mathrm{tr}})$ is the standard wavenumber for the whole atom + triatom system, defined by

$$k^2(E_{\mathrm{tr}}) = \frac{2M}{\hbar^2}E_{\mathrm{tr}}\,.$$

3. Numerical details

In this work, we have carried out quantum dynamical computations of nonreactive probabilities for the $O + HO_2$ collisional process over the range of translational energies 0.004–0.650 eV using the DMBE HO_3 potential energy surface of Varandas and Yu [1]. For its characterization, it may suffice to show in Fig. 2a contour plot diagram for the attacking oxygen atom moving coplanarly around the equilibrium HO_2 target molecule. We observe two minima associated with the terminal oxygen atom of the HO_2 radical and one in the vicinity of its central oxygen atom. Clearly, the potential energy surface is purely attractive when the atom attacks the molecule

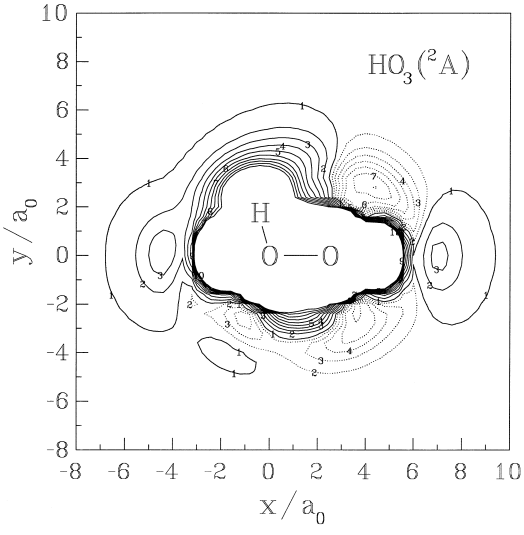

Fig. 2. Contour plot for an oxygen atom moving coplanarly around an equilibrium HO_2 radical. The solid contours start at -7.59206 eV (which corresponds to the $O+HO_2$ dissociation limit) and are equally spaced by 0.54423 eV. The dotted contours start also at -7.59206 eV and are separated by -0.27211 eV.

along certain nonlinear paths, although the remaining directions are seen to offer significant barriers before it can approach the molecule; we refer the reader to the original paper for further details.

The consecutive reactive probabilities have then been computed by means of Eq. (2) and wholly attributed to the reaction leading to $HO + O_2$ products. The calculations have generally been carried out within the j_z-approximation using a polar-averaged expression of the potential energy surface. However, in order to derive the perturbed part of the total wave function in the reagents' AC χ_{λ_0}, the parameter γ has been treated as an IOSA parameter. In agreement with Ref. [8] (see Fig. 2), it has been found that the reactive region of interest ranges for values of γ between 0 and 80 degree. The computed probabilities have then been numerically averaged as indicated in Eq. (18) by integration over $\cos\gamma$ and hence accounting for the appropriate weighting factors.

To solve Eq. (5) in an adequate way (for a given ψ_{λ_0}), the *R*-translational axis has been required to be divided into up to 180 equidistant sectors. In each of these one Gaussian, standing as a translational basis function and a set of twofold adiabatic vibrational basis functions have been used (see Eq. (14)). Since the OH bond behaves essentially like a spectator [8], it has been found that only one vibrational basis function along this axis was necessary to accurately describe the relaxation of this bond. The overall reactivity of the title process is carried out through the vibrations of the terminal O atom with the OH bond along ρ, (i.e. the center of mass atom-diatom vibrations). As expected from the observations in Ref. [8] where highly excited O_2 product molecules have been found to be formed, we needed at least 50–60 basis functions along ρ in order to correctly describe these twofold adiabatic vibrational basis functions. The number of such functions varies from one sector to another but at each sector their number is constrained by a simple energy value of 1.8eV [18,21]. This implied at the end, solving about 4000 complex equations in order to obtain the mentioned coefficients.

The most difficult task to implement was, nevertheless, the calculations using the average of the potential described in Eq. (7) due to the large anisotropy in β of the HO_3 DMBE potential energy surface. Indeed, a full consideration of Eq. (7) would force us to carry-out different convergence tests at each γ position, without mentioning the complexity that this anisotropy introduced in the tests. Thus, for simplicity, we have averaged the potential only over two positions, namely $\beta = 0$ and 180 degree (i.e. we have fully considered a coplanar configuration). Note that even if further β values were taken into consideration for the averaging procedure, this would still convert the real 6D problem in a pseudo coplanar one. Furthermore, an exact treatment of a coplanar reaction would require a 5D treatment to be fully resolved and hence our 3D study represents a reduced dimensionality analysis even for a coplanar situation. Thus, the averaging approximation used in this work should not drastically affect the essentials of the calculations and it has indeed also been frequently adopted by other authors [22–24].

4. IOSA results and novel elastic adiabatic optimum angle approach

Fig. 3 shows the calculated IOSA reactivity cross sections for the title reaction as a function of the

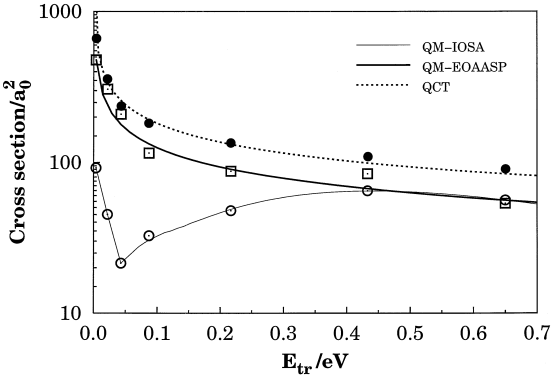

Fig. 3. A comparison of the cross section as a function of the translational energy for the process $O + HO_2 \rightarrow OH + O_2$ for the different theories mentioned in this Letter. Curves have been computed for values of E_{tr} ranging from 0.004 to 0.650eV.

translational energy. The results are presented for values of E_{tr} which range from 0.004 to 0.650 eV. Also given for comparison are the corresponding QCT values. The IOSA results show, on decreasing the collisional energy, a rapid decline of the computed cross section at first (as in recent publications [14–16]) and then a new feature not yet reported consisting of a sharp increase at low energies, which contrasts with the available QCT results. This may be due to the fact that the IOSA method sampled an angle close to that of the optimum path (see later) and due to the averaging procedure in Eq. (18) the final calculated cross section became very small. The fact that in the present case the QCT results at high energies are still larger than the IOSA ones may in turn be explained by the narrow cone of acceptance for the title reaction. Such a cone of acceptance definitely lowers, by virtue of the limitations imposed by Eq. (2) and Eq. (18), the expected values of the IOSA reactive cross sections. Conversely, the QCT theory is seen to direct more trajectories to the reaction region than those of a random distribution of $\cos\gamma$ in Eq. (18) would predict. This fact may be rationalized as due to a reorientation of the HO_2 molecule as the O atom approaches it, such as to find the optimum reaction pathway. This is a fair explanation due to the fact the incoming O atom tends to attack the terminal oxygen atom of the triatomic molecule and the atom H is light (thus, the HO_2 molecule can easily rotate to offer the terminal O atom to the homologous attacking one).

In order to make a more fair comparison between classical and quantum mechanical predictions, a correct distribution of $\cos\gamma$ is required in the QM calculations. For that purpose a four dimensional modelling of the QM theory for the title reaction is necessary, which is outside of the scope of this work. Indeed, we even doubt on its feasibility, given the present computing availabilities. Instead, always within the framework of a 3D QM calculation, we developed an alternative method which we named elastic optimum angle adiabatic single path (EOAASP). In this method, we imagine the process happening so slowly, that at any translational distance R, the HO_2 triatom molecule accommodates itself always to the angle γ that minimizes the potential energy surface. In a certain sense, it is the opposite approach to the IOSA and may a priori be considered as the upper most limit of the QM reactivity in a 3D treatment.

The angle γ_{EOAASP} is defined as the minimum of $\overline{U}(Rr_e\,\rho_e\,\theta_e\gamma)$ with respect to γ. In practice, it is determined by imposing the condition of extremum given by

$$\frac{\partial}{\partial\gamma}\overline{U}(Rr_e\,\rho_e\,\theta_e\gamma)|_{\gamma=\gamma_{EOAASP}} = 0 \qquad (20)$$

Although the requirement of a positive second-derivative has not been imposed, as it should mathematically, test calculations indicate that solving Eq. (20) is sufficient for practical purposes. However, it should be noted that this formula is useful only when there is one well defined stationary point along γ on the β-averaged potential energy surface. If this is not the case, the above procedure may lead in some cases to spurious features coming from the mixing of two or more different paths. Under such circumstances, we can find the optimum γ value for each value of the polar angle β and then average the calculated β-specific results over β. Such an optimum angle adiabatic multiple path (EOAAMP) approach will be further examined in current work for the $H + O_3$ reaction (this is known to have two attacking angles [15,16,25]). To keep consistency with the IOSA calculations of the present work, the optimum value of γ will be obtained as described in Eq. (20). The calculated values along the reaction path are shown in Fig. 4(a) as a function of the

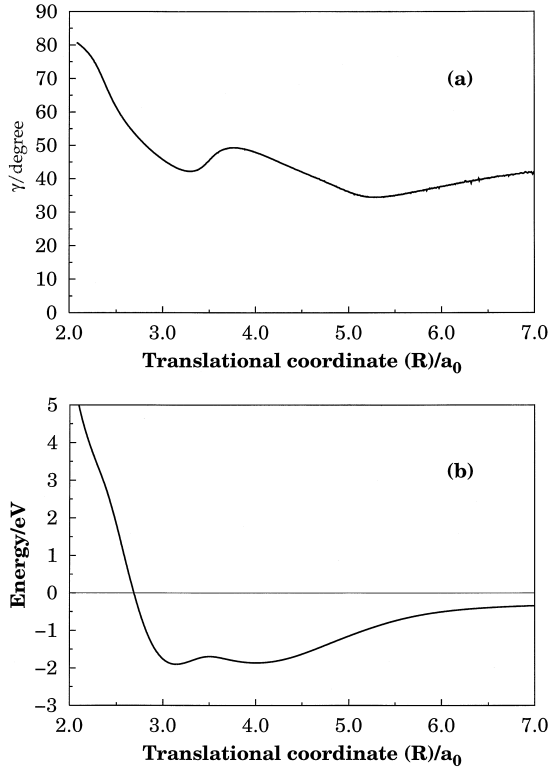

Fig. 4. Elastic optimum angle (EOAASP) adiabatic path: (a) optimum angle vs. translational distance R; (b) variation of the corresponding minimum energy as a function of R. The small ripples in panel (a) reflect some numerical noise in the optimization procedure.

translational distance R. The fact that it varies smoothly as R decreases gives us confidence that such a variation may be assumed as realistic. The corresponding variation of the minimum energy is illustrated in Fig. 4(b). Again, its behaviour looks smooth and acceptable, showing no barriers to the incoming O atom.

The treatment of the QM adiabatic path approach is completed by replacing the value of γ appearing in Eq. (2) through to Eq. (17) by the value of γ_{EOAASP} as defined in Eq. (20). Application of Eq. (18) is not necessary, since we require to carry out our calculations only once on a single optimum γ path.

Calculations obtained for the reactive cross sections in the title reaction using this last approach are also shown in Fig. 3 for comparison. Surprisingly, at high energies, both IOSA and EOAASP QM approaches give the same results, although they rely on opposite principles. This may suggest the fact that at high energies it is irrelevant the way that the path is chosen during the collisional process. Clearly, the EOAASP method gives better agreement with the QCT theoretical predictions at lower energies and follows the typical capture type behaviour. As stated in previous publications, the fact that the QCT values exceed the QM EOAASP ones may partly be due to zero-point energy leakage which is not present, of course, in the QM calculations. Of course, we should recall that both the QCT and QM approaches used in the present work are approximate theories.

Fig. 5 shows the calculated thermal rate coefficients as a function of temperature over the range $100 \leq T/\mathrm{K} \leq 1700$. Also included for comparison are the results from available experimental measurements [4–7,26–30] and the QCT calculations [8] based on the same HO_3 DMBE potential energy surface. As usual, the rate coefficients of Fig. 5 have been calculated from the computed cross sections σ^r shown in Fig. 3 by using the formula

$$k(T) = f(T)\left(\frac{8k_BT}{\pi M}\right)^{1/2}\left(\frac{1}{k_BT}\right)^2 \times \int_0^\infty E_{\mathrm{tr}}\,\sigma^r \exp(-E_{\mathrm{tr}}/k_BT)\,\mathrm{d}E_{\mathrm{tr}} \qquad (21)$$

where M is the reduced mass of the atom-triatom colliding pair, k_B is the Boltzmann constant and

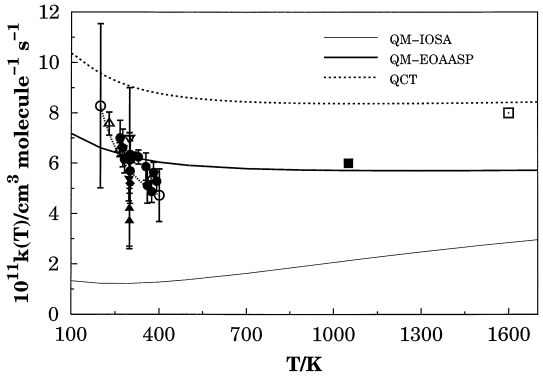

Fig. 5. Logarithmic plot of the rate constant as a function of T: solid line, QM IOSA results; thin line, QM EOAASP results; dotted line QCT results. The remaining symbols indicate experimental results [26,5,27,6,4,7,28–30].

$f(T)$ is the appropriate electronic degeneracy factor, which for the title reaction adopts the form

$$f(T) = \frac{1}{5 + 3\exp\left(-\frac{227.6}{T}\right) + \exp\left(-\frac{325.9}{T}\right)} \tag{22}$$

where T is expressed in kelvin (K). Note that Eq. (22) accounts for the electronic degeneracies of $O(^3P) + HO_2(^2A'')$ and the fact that the DMBE potential energy surface refers to $HO_3(^2A)$ [1,8,31,32]. To solve Eq. (21), we have first fitted the calculated σ^r of Fig. 3 to a suitable analytical form. These cross sections are, in the case of the IOSA method, well described by an expression of the form

$$\sigma^r_{\mathrm{IOSA}} = \frac{C_1}{E^{n_1}} + C_2 E^{n_2} \exp(-m_1 E) \tag{23}$$

while the EOAASP ones are best fitted using

$$\sigma^r_{\mathrm{EOAASP}} = \frac{C_3}{E^{n_3}} \exp(-m_2 E) \tag{24}$$

The different parameters C_i, n_i and m_i in Eq. (23) and Eq. (24) are given in units such that with E in eV the cross section comes in units of a_0^2. The fitting of the parameters C_i, n_i and m_i has been done by a trial-and-error procedure using the χ^2-criterion as an indicator for the optimum choice of these parameters. The following values have been obtained in the IOSA case: $C_1 = 6.455$; $n_1 = 0.4827$; $C_2 = 1925$; $n_2 = 2$ and $m_1 = 4.349$. In turn, for the EOAASP method, we have obtained $C_3 = 64.751$; $n_3 = 0.365$ and $m_3 = 0.6448$. The corresponding fitted curves are also shown in Fig. 3 for comparison.

5. Conclusions

We have carried out three-dimensional quantum dynamics calculations of the reaction $O + HO_2 \rightarrow HO + O_2$ using a recently reported [1] DMBE potential energy surface for the ground electronic state of HO_3. Two different concepts have been applied in developing the QM models. One, the IOSA approach, led to too low values of rate constant and cross sections, especially near the threshold. The other, developed from adiabatic considerations, yielded results in fairly good agreement with the available experimental data and also in reasonable agreement with previous QCT results. It is perhaps too soon to decide whether these results are sufficient for an assessment of the novel EOAAS(M)P approaches. More applications to other systems would be valuable for a more definite judgement.

Acknowledgements

This work has been supported by the Fundação para a Ciência e Tecnologia, Portugal, under programme PRAXIS XXI. HS is on leave from the Department of Physics and Applied Mathematics, Soreq NRC, Yavne 81800, Israel.

References

[1] A.J.C. Varandas, H.G. Yu, Mol. Phys. 91 (1997) 301.
[2] P. Crutzen, Science 277 (1997) 1951.
[3] J.I. Steinfeld, J.S. Francisco, W.L. Hase, Chemical Kinetics and Dynamics, Prentice-Hall, Englewood Cliffs, NJ, 1989.
[4] U.C. Sridharan, L.X. Qiu, F. Kauman, J. Phys. Chem. 86 (1982) 4469.
[5] L.F. Keyser, J. Phys. Chem. 86 (1982) 3439.
[6] A.R. Ravishankara, P.H. Wine, B.M. Nicovich, J. Chem. Phys. 78 (1983) 6629.
[7] W.H. Brune, J.J. Schwab, J.G. Anderson, J. Phys. Chem. 87 (1983) 4503.
[8] W. Wang, R. González-Jonte, A.J.C. Varandas, J. Phys. Chem. (1998) in press.
[9] H. Szichman, M. Baer, Chem. Phys. Lett. 242 (1995) 285.
[10] P. McGuire, D.J. Kouri, J. Chem. Phys. 60 (1974) 2488.
[11] R. T Pack, J. Chem. Phys. 60 (1974) 633.
[12] H. Szichman, A.J.C. Varandas, M. Baer, Chem. Phys. Lett. 231 (1994) 253.
[13] H. Szichman, A.J.C. Varandas, M. Baer, J. Chem. Phys. 102 (1995) 3474.
[14] H. Szichman, M. Baer, J. Chem. Phys. 105 (1996) 10380.
[15] H. Szichman, M. Baer, A.J.C. Varandas, J. Phys. Chem. 101 (1997) 8817.
[16] H. Szichman, M. Baer, A.J.C. Varandas, J. Phys. Chem., submitted for publication.
[17] D. Neuhauser, M. Baer, J. Chem. Phys. 90 (1989) 4351.
[18] H. Szichman, M. Baer, J. Chem. Phys. 101 (1994) 2081.
[19] M.R. Pastrana, L.A.M. Quintales, J. Brandão, A.J.C. Varandas, J. Phys. Chem. 94 (1990) 8073.
[20] H. Szichman, I. Last, A. Baram, M. Baer, J. Phys. Chem. 97 (1993) 6436.
[21] I. Last, A. Baram, H. Szichman, M. Baer, J. Phys. Chem. 97 (1993) 7040.
[22] D.C. Clary, J. Chem. Phys. 96 (1992) 3656.

[23] D.C. Clary, Chem. Phys. Lett. 192 (1992) 34.
[24] D. Wang, J.M. Bowman, Chem. Phys. Lett. 207 (1993) 227.
[25] H.G. Yu, A.J.C. Varandas, J. Chem. Soc. Faraday Trans. 93 (1997) 2651.
[26] J.M. Nicovich, P.H. Wine, J. Phys. Chem. 91 (1987) 5118.
[27] W. Hack, A.W. Preuss, F. Temps, H.Gg. Wagner, Ber. Bunsenges. Phys. Chem. 83 (1979) 1275.
[28] R.R. Lii, M.C. Sauer Jr., S. Gordon, J. Phys. Chem. 84 (1980) 817.
[29] J. Peeters, G. Mahnen, Symp. (Int.) Combust. 14 (1972) 133.
[30] M.J. Day, K. Thompson, G. Dixon-lewis, Symp. (Int.) Combust. 14 (1972) 47.
[31] S.R. Langhoff, R.L. Jaffe, J. Chem. Phys. 71 (1979) 1475.
[32] B.R. Johnson, N.W. Winter, J. Chem. Phys. 66 (1977) 4116.